Limnol. Oceanogr., 55(4), 2010, 1723–1732

doi:10.4319/lo.2010.55.4.1723

The relationship between near-surface turbulence and gas transfer velocity in freshwater systems and its implications for floating chamber measurements of gas exchange

Dominic Vachon,[a,*] Yves T. Prairie,[a] and Jonathan J. Cole[b]

[a] Département des Sciences Biologiques, Université du Québec à Montréal, Montréal, Québec, Canada
[b] Institute of Ecosystem Studies, Cary Arboretum, Millbrook, New York

Abstract

We performed a series of gas exchange measurements in 12 diverse aquatic systems to develop the direct relationship between near-surface turbulence and gas transfer velocity. The relationship was log-linear, explained 78% of the variation in instantaneous gas transfer velocities, and was valid over a range of turbulent energy dissipation rates spanning about two orders of magnitude. Unlike wind-based relationships, our model is applicable to systems ranging in size from less than 1 km^2 to over 600 km^2. Gas fluxes measured with our specific model of floating chambers can be grossly overestimated (by up to 1000%), particularly in low-turbulence conditions. In high-turbulence regimes, flux overestimation decreases to within 50%. Direct measurements of turbulent energy dissipation rate provide reliable estimation of the associated gas transfer velocity even at short temporal and spatial scales.

Gas exchange at the air–water interface is central to any attempt to establish a credible carbon budget, whether at a local, regional, or even global scale. While this is particularly obvious for marine systems, inland waters have recently been shown to have a larger-than-expected role in this regard (Cole et al. 2007). However, the physical processes modulating gas exchange with the atmosphere are complex and are currently modeled only with great uncertainty (Frost and Upstill-Goddard 2002; Zappa et al. 2007). Consequently, accurate carbon emission estimations are difficult to achieve. For nonreactive gases, gas exchange can be adequately modeled as a Fickian diffusive process and is therefore driven by two variables: the difference in gas partial pressure between the air and the water and the gas transfer velocity (k). For gases of low solubility in water, such as O_2 or CO_2, dissipation via the mass boundary layer will be the main transfer, such that

$$F = k \times Kh(p\mathrm{X}_{\mathrm{water}} - p\mathrm{X}_{\mathrm{air}}) \quad (1)$$

where F is the flux of a slightly soluble gas X across the air–water interface, k is the gas transfer velocity at a given temperature, Kh is the Henry's coefficient (corrected for salinity and temperature), and $p\mathrm{X}_{\mathrm{water}}$ and $p\mathrm{X}_{\mathrm{air}}$ are the gas partial pressures in water and air, respectively.

Since both the atmospheric and aqueous CO_2 partial pressure can now be easily measured in the field (Cole and Prairie 2009), the main challenge in applying Eq. 1 is to estimate accurately the gas transfer velocity k. All processes affecting the mass boundary layer condition will mediate gas transfer velocity. It is known that for poorly soluble gases such as CO_2 and O_2, water side near-surface turbulence is the main driver of gas transfer velocities across the air–water interface (MacIntyre et al. 1995). The coupling between turbulence and gas transfer velocity was originally derived from surface renewal theory (Dankwerts 1951). By constantly renewing the surface mass content with small eddies, turbulence thereby enhances the rate of diffusive gas exchange. More specifically, the gas transfer velocity k was shown to be directly related to near-surface turbulence from the characteristics of viscous eddies (Lamont and Scott 1970), as follows:

$$k \propto (\varepsilon \upsilon)^{1/4} Sc^{-n} \quad (2)$$

where ε is the turbulent kinetic energy (TKE) dissipation rate, υ is the kinematic viscosity of water, Sc is the Schmidt number, and k is the gas transfer velocity. Depending on the surface contamination, n will vary from 1/2 to 2/3. Because ε varies with depth, this relationship holds only if ε is measured at the interface of interest (i.e., near the surface). This theoretical relationship has been recently examined in natural systems (Zappa et al. 2007; Tokoro et al. 2008) and was found to hold generally.

The relationship between turbulence and gas exchange is also the basis for the many empirical functions relating k to wind speed, where wind speed is used as an integrative proxy for turbulence (Wanninkhof 1992; Wanninkhof and McGillis 1999). However, the existence of a unique and universal wind–k relationship for all systems is highly questionable given that for any wind speed, its effect on gas exchange is unlikely to be the same in the ocean and, for example, in a small kettle lake. Moreover, many studies have shown that other factors will affect k, such as wind fetch (Frost and Upstill-Goddard 2002; Borges et al. 2004; Guérin et al. 2007), tidal currents (Borges et al. 2004; Zappa et al. 2007), rainfall (Ho et al. 1997, 2007), microscale breaking waves (Zappa et al. 2004), thermal convection (Schladow et al. 2002; Eugster et al. 2003), organic matter or suspended matter (Abril et al. 2009; Calleja et al. 2009), and surfactants (Frew et al. 1990; McKenna and McGillis 2004).

Establishing a reliable relationship between turbulence and k assumes that both variables can be measured accurately and precisely. While there is consensus that modern instruments such as acoustic Doppler velocimeters

* Corresponding author: vachon.dominic@courrier.uqam.ca

can measure turbulence precisely even at microscales, methods to measure k are numerous and more diverse, although they basically all rely on inverting Eq. 1 to isolate k and measuring the other variables in the field, namely the gas partial pressure gradient and the flux. In practice, what varies among methods is the degree of time and space integration in the measured fluxes, and this variance can often lead to differing results. At one extreme, gas tracer experiments that typically use sulfur hexafluoride (SF_6) provide the widest spatial (a few square kilometers) and temporal (days to weeks) integration. However, they are cumbersome to repeat in multisystem studies or over different time periods. They are often inadequate if the purpose of the study is to examine the effects of other environmental characteristics (such as rain or surfactant concentration), which themselves vary on shorter scales than the integration scale, over which the gas tracer experiment takes place. An alternative approach consists of continuously measuring gas fluxes using the eddy covariance technique over a footprint area of typically a few hundred square meters, depending on the height of the tower. While this approach is highly promising, it remains currently expensive and technically difficult, and, again, it is impractical for the study of several systems. At the other extreme, highly localized (less than 0.5-m^2) and nearly instantaneous CO_2 fluxes can be measured directly with floating chambers (FCs) (Frankignoulle 1988). This technique is simple, inexpensive, and highly portable. However, FC-derived fluxes are problematic as well. Some authors (Eugster et al. 2003; Kremer et al. 2003; Matthews et al. 2003) have shown that fluxes measured by FCs are higher than those obtained from SF_6 additions, from the often-used wind–k parameterization, and from the 'eddy covariance' method. Other authors (Guérin et al. 2007; Repo et al. 2007; Soumis et al. 2008) have shown that FC measurements yield values consistent with those of other methods.

There are several reasons why FCs may be overestimating true fluxes. First, the FC causes mass boundary layer perturbations and will thus affect the flux measurement (Kremer et al. 2003; Lambert and Fréchette 2005). Second, by disturbing the air–water interface, the FC generates artificial turbulence inside the sampling area. The chamber moves slightly but constantly on the surface water, even under very weak winds, and the chamber's walls induce artificial turbulence. Matthews et al. (2003) suggest that FCs with edges (or a skirt) at the same level as the water surface tend to overestimate fluxes by up to a three- to fivefold measure as compared to chambers with longer edges that enter the water.

Whether one is fundamentally interested in elucidating the factors driving variations in k or whether one is concerned with measuring k with minimum bias, the relationship between in situ turbulence and gas exchange is the nexus. The aim of this study was thus to explore and quantify the direct link between k and near-surface small-scale turbulence in a series of freshwater systems of different characteristics, both natural and man-made. We then hypothesized that if gas transfer velocities are driven mainly by near-surface turbulence, in situ turbulence could be used to estimate the gas transfer velocity directly. Also, as a secondary objective, we assessed the commonly held view that FCs tend to overestimate gas fluxes because of the artificially created turbulence within the sampling area. Our ultimate goal is to develop methods of estimating in situ the local gas transfer velocity either without FCs or by providing appropriate correction factors that minimize chamber-induced biases.

Methods

Study areas—Samples were taken from two different regions of Québec (Canada). First, as part of a larger project evaluating the net effect of reservoir impoundment on the carbon balance of the landscape relative to the undisturbed conditions, we collected samples from the Eastmain-1 hydroelectric reservoir (602 km^2) located near James's Bay, Québec, Canada (52°7′N, 75°58′W). The sampling campaigns (one in late July and a second in early September 2008) were planned to provide great variability in weather conditions, particularly wind speed. Second, in order to sample a wider range of system types, 11 lakes located in the Eastern Township region (Québec, Canada; 45°20′N, 72°5′W) were also sampled (n = 23) during August 2008 and were chosen to cover a wide variability in size (lake surface areas ranging from 0.2 to 11.7 km^2 and average depths ranging from 0.8 to 17.7 m) and biological productivity. For the Eastmain-1 reservoir (ER) samples (n = 98), sites were chosen near an eddy covariance tower placed on a small island. For Eastern Township lakes (ETL), samples were taken at the deepest point of the lakes.

Gas transfer velocity for Schmidt number of 600 (k_{600}) calculations and associated measurements—This method comprises an enclosed chamber (surface area: 0.1 m^2) fitted with floats set over water in which the rate of CO_2 accumulation is measured. The compartment was made of a plastic storage bin covered with aluminum paper to minimize temperature modulation inside the chamber over the short time period (10 min) required to obtain good results. Floating devices were placed on the sides to ensure a constant volume of 23 liters when deployed and to allow 6 cm of the wall extensions to penetrate the water column. The enclosed chamber was connected to an infrared gas analyzer (IRGA; PPSystem, EGM-4) via tygon tubing (inner diameter: 3.175 mm) in a closed recirculating loop with an in-line moisture trap (drierite) located just before the gas analyzer. The IRGA calibration was checked before each sampling campaign with a standard analyzed gas (CO_2 at 618 ± 12 μatm) and was shown to be within the stated accuracy range (less than 1% of the span concentration). The detection limit of the gas analyzer is less than 5 μatm, which is well below the lowest CO_2 partial pressure (pCO_2) sampled in this study. The chamber was flushed with ambient air prior to each measurement.

The partial pressures of CO_2 were recorded every minute for 10 min, and the rate of accumulation was computed by linear regression. Although 95% of the chamber measurements had linear increases with $R^2 > 0.95$, flux measurements were rejected when R^2 was less than 0.90. For

purposes of calculating gas transfer velocity, surface-water pCO_2 was determined by pumping water from a depth of about 10 cm (with a peristaltic pump) through a gas equilibrator (membrane contactor MiniModule) coupled to an IRGA in a closed recirculating loop (Cole and Prairie 2009). Laboratory tests indicated a half-equilibration time of ~ 4–5 s. Nevertheless, we always waited 1 min to allow full equilibration and therefore did not require correction. Floating chamber measurements were made in blocks of four measurement series, taking water pCO_2 and temperature at the beginning and at the end of each block and at the same position in which the floating chambers were deployed.

With the resulting measured fluxes (FCO_2), surface-water pCO_2, and atmosphere pCO_2, k_{CO_2} was calculated by inverting Eq. 1 as follows:

$$k_{CO_2} = \frac{F_{CO_2}}{Kh(pCO_{2_{water}} - pCO_{2_{air}})} \quad (3a)$$

which was then standardized to a Schmidt number of 600 using

$$k_{600} = k_{CO_2}\left(\frac{600}{Sc_{CO_2}}\right)^{-n} \quad (3b)$$

where Sc_{CO_2} is the CO_2 Schmidt number for a given temperature (Wanninkhof 1992; Kremer et al. 2003). We used $n = 2/3$ for wind speed < 3.7 m s^{-1} and $n = 1/2$ for wind speed > 3.7 m s^{-1} (Guérin et al. 2007).

Turbulent kinetic energy dissipation rate (ε)—Of the many possible metrics of turbulence, ε was chosen because of its particular suitability on the Lagrangian reference frame that was used in this study. ε values were calculated using the inertial range method from three-dimensional water velocity time series. When the surface water is isotropic and the turbulence is fully developed, eddies break up into smaller eddies to dissipate completely. This phenomenon can be seen on a density spectrum of the fluctuating current velocities according to Kolmogorov's law:

$$P_{(k)} = \alpha\varepsilon^{2/3}\kappa^{-5/3} \quad (4)$$

where $P_{(k)}$ is the wave number spectrum of the fluctuating current velocities, α is Kolmogorov's empirical constant (0.52, according to Zappa et al. [2003]), and κ is the wave number. We can assume Taylor's hypothesis of frozen turbulence if the turbulent motions are 'slow' (i.e., a long dynamical time) relative to the time required to convect them past the probe. Because our turbulence measurements followed a Lagrangian reference frame relative to the mean flow, we used the mean wave orbital velocity as the advective velocity (V). Kitaigorodskii et al. (1983) suggested the criterion $(u/V)^3 < 1$ to assess the adequacy of the frozen turbulence hypothesis, where u is the root mean square (RMS) of fluctuating velocities. In all of our cases, this criterion was on average less than 0.015, ranging from 0.002 to 0.2. Thus, we derived the wave number spectra from the frequency spectra of the current velocities time series by $\kappa = 2\pi f/V$, where f is the frequency and V is the advective velocity, the mean wave orbital velocity.

To measure current velocity fluctuations, we used an Acoustic Doppler Velocimeter (ADV; Sontek 10 MHz) at 25 Hz during a period of 10 min for each sample. The quality of the time series was first tested by checking whether the signal-to-noise ratio was greater than 15 db and whether the correlation between studs was greater than 70%. Data rejected according to these criteria were replaced by the mean velocity. In addition, data that were different by over three times the standard error were also replaced by the mean velocity. Power spectra were then produced from the time series using the *pwelch* function (MATLAB 7.1). Because turbulence is considered a three-dimensional isotropic, either vertical or horizontal velocities could be used for spectral analysis. In this study, horizontal current velocities were selected because they showed the greatest consistency. The range of frequency used for calculation of ε varied between 3 and 6 Hz to avoid the interference generated by unwanted distortion, such as that produced by the wave-induced movements of the ADV at lower frequencies (Lumley and Terray 1983). As the integration of the power spectra over the entire range of frequencies necessarily represents the variance of the associated velocity measurements (from which an RMS value can be obtained), we calculated the mean wave orbital velocity (V) by integrating the power spectrum of vertical velocities over the region associated with the wave motion (i.e., the hump, between 0.8 and 2.5 Hz). Our V values varied between 0.04 and 0.63 m s^{-1}.

Evaluating the FC method—To evaluate the claim that the FC method tends to overestimate gas fluxes because of artificially enhanced turbulence created by the chamber movements, we duplicated our flux and turbulence measurements under two different configurations. In all cases, the ADV was placed in the water horizontally with a Lagrangian floating structure at a constant sampling depth of 10 cm. In one configuration, the floating structure was positioned such that the ADV would measure directly underneath the center of the FC (*see* Fig. 1). In the second configuration, the ADV was positioned sideways to measure turbulence about 25 cm outside the perimeter of the chamber. The samples were thus separated in two sets, inside FC measurements and free water, slightly outside the chamber (ε_{in} and ε_{fw}, respectively). Our working hypothesis is that the relationship between k_{600} and ε_{in} should represent the true relationship between turbulence and gas transfer velocity, even if they are both artificially inflated. Moreover, if FCs do create artificially turbulent regimes, then the data from the k_{600} vs. ε_{fw} should fall above the line of best fit of the k_{600}–ε_{in} relationship because the ε_{fw} would not be compromised by FC-induced turbulence. Thus, the extent of the departure between the k_{600}–ε relationships under the two measurement configurations describes the degree of overestimation induced by FCs and can therefore be used as a general correction factor.

Meteorological data—Wind speed measurements were taken on site before and after each FCs using a hand-held

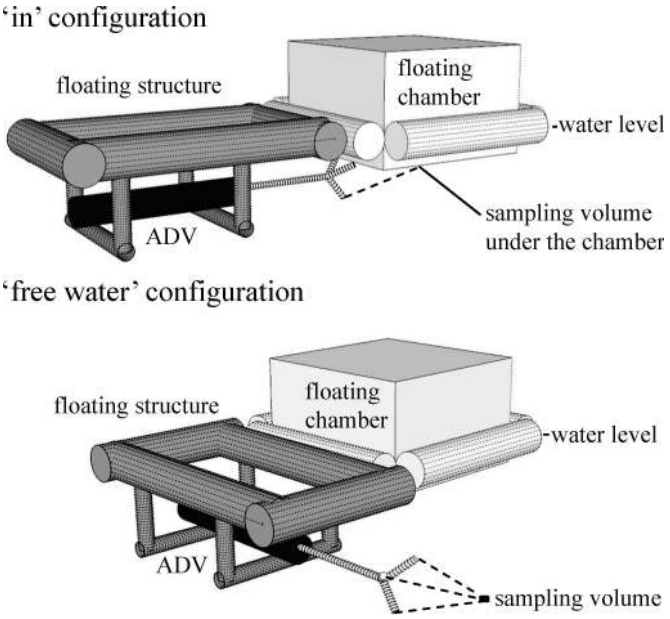

Fig. 1. Sampling setup for measuring near-surface turbulence with the ADV inside the floating chamber (i.e., 'in' configuration, ε_{in}), directly below the sampling area and the free-water turbulence measurement setup (i.e., 'free water' configuration, ε_{fw}). Turbulence sampling was always at 10 cm in depth.

anemometer (Kestrel 4000, accuracy 3% of reading, response time of 1 s and operational range of 0.3–40 m s^{-1}) at 1 m above the water surface. The two measures during 1 min were then averaged to produce a representative wind speed associated with each FC measurement. We extrapolated the wind speed data to wind speed at 10 m (U_{10}) according to the logarithmic wind profile relationship of Crusius and Wanninkhof (2003), thus:

$$U_{10} = U_z \left[1 + \frac{(C_{d10})^{1/2}}{\kappa} \ln\left(\frac{10}{z}\right) \right] \quad (5)$$

where z is the measured wind speed height, C_{d10} is the drag coefficient at 10 m in height (0.0013; Stauffer 1980), and κ is the Von Karman constant (0.41). We also used the hand-held anemometer to measure air temperature (± 0.5°C). Wave height was coarsely estimated using a graduated stick.

Results

Wind speed and other meteorological parameters—Table 1 summarizes the data from the different campaigns in the ER and ETL in August 2008. Reservoir meteorological variables showed a wider range than did ETL. Mean wind speed at 10 m high (U_{10}) at the ER site was 3.8 ± 1.7 m s^{-1} (mean ± SE, n = 98), ranging from 0.0 to 8.8 m s^{-1}, slightly lower than the mean of 4.0 ± 1.3 m s^{-1} (mean ± SE, n = 23), ranging from 1.9 to 6.6 m s^{-1}, for ETL sites. The average wind speed standard deviation between the before and after FC measurements was 0.5 m s^{-1} (n = 118). The reliability of the hand-held wind speed measurements was assessed when our sampling sites were in close proximity to an eddy covariance tower equipped with a sonic anemometer, and those were found to agree well. Mean air temperatures were 15.5°C ± 3.9°C (mean ± SE, n = 98, range: 7.4–28.0°C) and 19.5°C ± 2.8°C (mean ± SE, n = 23, range: 13.9–23.3°C) for the ER and ETL sites, respectively.

Gas transfer velocities (k_{600})—We estimated the precision of our gas transfer velocities data from first-order error propagation formulas based on the uncertainties of the water pCO_2 measurements and of the slope of the time accumulation rate of CO_2 inside the chamber. Beginning and ending pCO_2 measurements were always within 5% of variation of each other. For the ER sites, 90% of the data had a coefficient of variation (CVs) of less than 15%. For ETL sites, 75% of the data set had a CV of less than 20%. In both cases, most (about 80–85%) of the uncertainty in the k_{600} values obtained was due to variations in the partial pressure differential, while the remainder was due to uncertainty in the CO_2 accumulation rate. The slightly greater variation in our k_{600} values obtained from the ETL sites is likely attributable to the generally lower fluxes observed and the corresponding higher relative error of the regression slopes of CO_2 accumulation in the chambers. The average value of gas transfer velocities (k_{600}) on the ER site was 18.8 ± 6.7 cm h^{-1} (mean ± SE, n = 98, range: 3.7–31.7 cm h^{-1}), and 15.8 ± 4.8 cm h^{-1} (mean ± SE, n = 23) ranging from 8.4 to 26.5 cm h^{-1} for lakes (Table 1). The sampling conditions considered by Kremer et al. (2003) to be suitable for FC measurements were always met in our study: wind condition speed was below 8 m s^{-1}, and wave height was never high enough to break the seal between the chamber and the water surface (average wave height was 0.13 ± 0.11 m). Similarly, although whitecaps were not quantified, their rare occurrence and low magnitude would not have influenced our chamber measurements, particularly in view of the fact that we never found inconstancies in the linearity of gas accumulation rate within the FCs. We thus contend that our FC was used within the limits suggested by Kremer et al. (2003).

ε and its relationship to gas transfer velocities—Dissipation rates were derived from the adequacy of the −5/3 slope fitting of the Kolmogorov's law on the power spectrum of the horizontal velocities (example shown in Fig. 2). The vast majority of the spectra showed a clear hump around 1.3 Hz, which represents the relative vertical motion of our measuring system. Some measurements were excluded when the spectrum was visibly not following the expected slope. On this basis, only 10% of the ε values were excluded in the ER data set, but 30% of the values from the ETL were excluded. We suggest that the higher exclusion in the ETL region is attributable to the very low turbulence (wind) we often encountered there, making energy dissipation rate more difficult to measure. The overall range in free-water TKE dissipation rate (ε_{fw}) spanned nearly two orders of magnitude among our samples and sites and ranged from 5.4×10^{-6} to 7.5×10^{-5} m^2 s^{-3} and from 8.3

Table 1. General data set of the main variables measured on field.* They are separated in three sampling campaigns: July 2008 on the Eastmain-1 reservoir (ER); August 2008 on several lakes in the Eastern Township (ETL) area; and September 2008, again on the ER.

	Site		
	ER	ETL	ER
Sampling period	Jul 2008	Aug 2008	Sep 2008
fCO_2 (mmol m^{-2} d^{-2})	92.7±46.0(41)	61.2±62.2(23)	166.7±66.1(57)
ΔpCO_2 (μatm)	529±122(41)	429±477(23)	895±59(57)
k_{600} (cm h^{-1})	17.7±6.2(41)	15.8±4.8(23)	19.5±7.0(57)
U_{10} (m s^{-1})	3.3±0.9(41)	4.0±1.3(23)	4.2±2.0(57)
Wave height (m)	0.10±0.08(37)	0.05±0.04(17)	0.17±0.13(57)
Air temp. (°C)	17.8±2.8(41)	19.5±2.8(23)	13.8±3.7(57)
Water temp. (°C)	18.7±0.6(41)	21.0±0.8(23)	16.4±0.8(57)
ε_{in} (m^2 s^{-3})	$1.1\times10^{-4}\pm6.7\times10^{-5}$(21)	$1.1\times10^{-4}\pm9.6\times10^{-5}$(8)	$1.7\times10^{-4}\pm1.3\times10^{-4}$(28)
ε_{fw} (m^2 s^{-3})	$3.1\times10^{-5}\pm1.8\times10^{-5}$(20)	$2.2\times10^{-5}\pm1.5\times10^{-5}$(15)	$3.5\times10^{-5}\pm1.4\times10^{-5}$(29)

* Mean ± standard error, with n in parentheses; fCO_2, CO_2 flux across the air–water interface; ΔpCO_2, CO_2 partial pressure difference between water and atmosphere; k_{600}, gas transfer velocity for the Schmidt number of 600; U_{10}, wind speed at 10 m high; Air temp., ambient air temperature; water temp., surface-water temperature; ε_{in}, turbulent kinetic energy dissipation rate measured inside the FC sampling area; ε_{fw}, turbulent kinetic energy dissipation rate measured in free water near the FC.

$\times 10^{-6}$ to 5.4×10^{-5} m^2 s^{-3} for the ER and ETL sites, respectively. These values are comparable to those of the upper mixed layer of other lakes (MacIntyre et al. 1995) but lower than dissipation rates found under breaking wave conditions (Terray et al. 1996), in estuaries with tidal currents (Zappa et al. 2007), or in the turbulent coastal environment (Tokoro et al. 2008). TKE dissipation rate inside the FC (ε_{in}) averaged $1.5 \times 10^{-4} \pm 1.1 \times 10^{-4}$ m^2 s^{-3} (mean ± SE, $n = 49$) at the ER site and $1.1 \times 10^{-4} \pm 9.6 \times 10^{-5}$ m^2 s^{-3} (mean ± SE, $n = 9$) in ET lakes (Table 1).

The relationship between turbulence and gas transfer velocities was first examined using only the measurement pairs, with the turbulence measurements taken just 10 cm under the FC (i.e., the 'in' configuration). Figure 3 shows the significant relationship between k_{600} and ε_{in}. Least-squared linear regression analysis produced the predictive equation ($R^2 = 0.78$, $n = 57$, $p < 0.0001$)

$$k_{600} = 78.22\,(\pm 4.25) + 14.66\,(\pm 1.05)\log_{10}\varepsilon_{in} \qquad (6)$$

where k_{600} is measured in cm h^{-1} and TKE dissipation rate (ε_{in}) in m^2 s^{-3}. Note that turbulence measurements are log transformed and that the intercept cannot therefore be interpreted as the k_{600} value at no turbulence. When applying our ε_{in} measurements to the small-eddy model (Eq. 2), our data showed a remarkable correspondence with theory (Fig. 4). According to this model, the regression slope between the observed and small-eddy modeled k_{600} values must pass through the origin and be linear, with both of these conditions visibly fulfilled. Furthermore, an analysis of covariance (ANCOVA, $p > 0.05$) showed that the parameters of this relationship are not different between lakes and the reservoir, emphasizing the generality of the model for freshwater systems ranging in size from 0.20 km^2 to over 600 km^2.

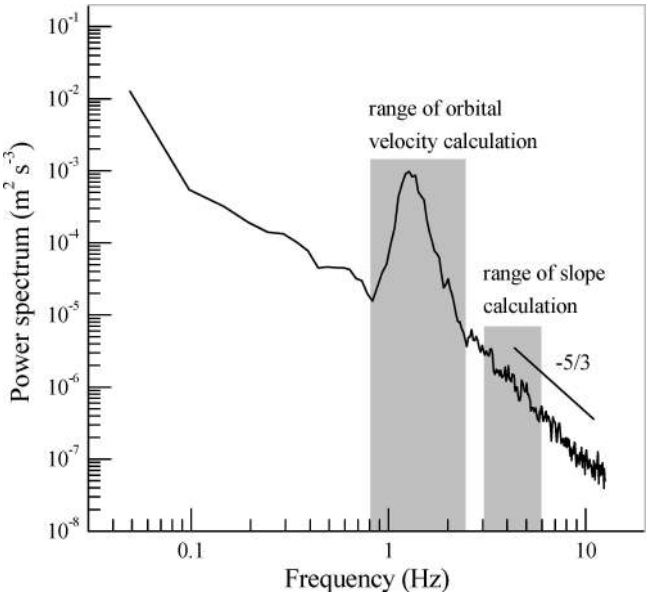

Fig. 2. Power spectrum of the horizontal current fluctuation measured with ADV. Solid straight line is the −5/3 slope on a log–log scale according to Kolmogorov's law, which was used for TKE dissipation rate (ε) calculation. The frequency range used in our calculations ranged from 3 to 6 Hz. Peak around 1.3 Hz corresponds to the wave motion. Consequently, anything below this range was not used in the calculations.

FC method: biases and corrections—Because a single ADV instrument was available, inside FC and free-water turbulence measurements were made sequentially, thus precluding a direct and simultaneous comparison of turbulence inside and outside of the chamber. Instead, we evaluated the potential bias by comparing the parameters describing the relationship between k_{600} and ε in the two measurement configurations. If FCs do not induce bias by modifying turbulence, the two relationships should be the same.

As was the case for the turbulence data obtained just under the FCs (in configuration, Fig. 3), we found a similarly significant relationship between k_{600} and ε_{fw} (Fig. 5; $R^2 = 0.48$, $n = 64$, $p < 0.0001$) for the data in the 'free-water' configuration. However, the position of most of our observations fell above the best-fit line obtained earlier (Eq. 6 and dashed line in Fig. 5), implying

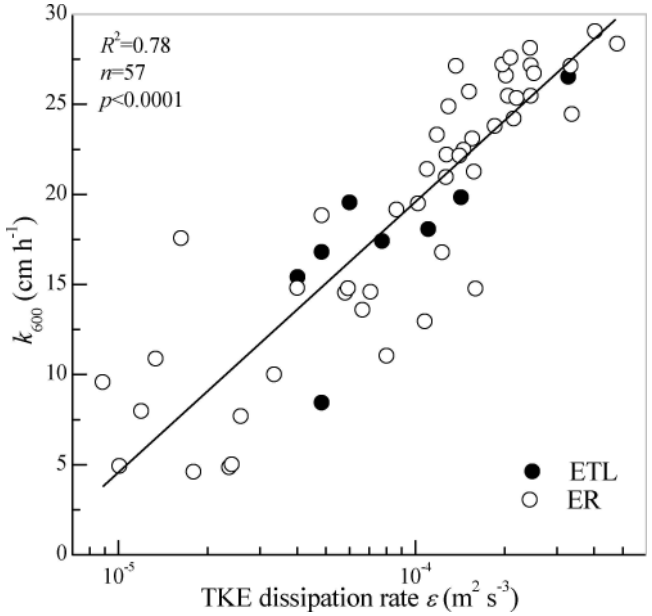

Fig. 3. Least-square linear regression between turbulent kinetic energy dissipation rates inside the FC (ε_{in}) and associated FC k_{600} values for ER and ETL data [k_{600}=78.22 (± 4.25) + 14.66 (± 1.05)$\log_{10}\varepsilon_{in}$], $R^2 = 0.78$, $n = 57$, $p < 0.0001$.

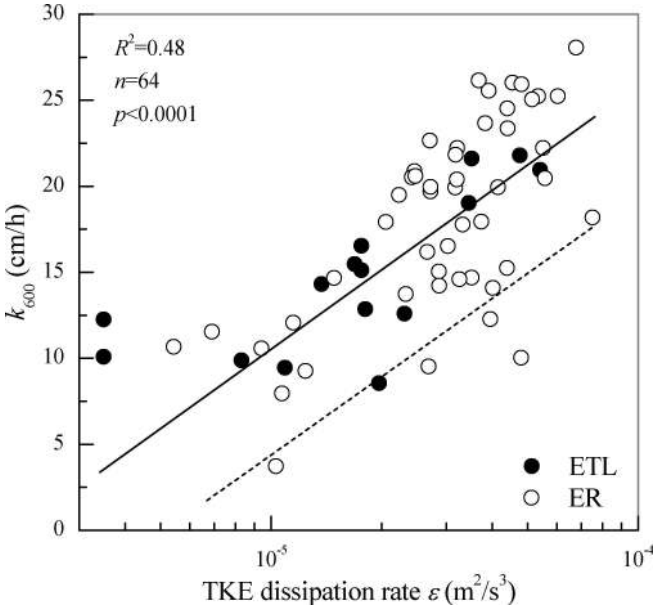

Fig. 5. Solid line represents the relationship between free-water measurements (ε_{fw}) and measured k_{600} with FC (k_{600} = 77.96 [± 7.99] + 13.21 [± 1.74] $\log_{10}\varepsilon_{fw}$, $R^2 = 0.48$, $n = 64$, $p < 0.0001$). The dashed line is the relationship between ε_{in} and k_{600} (Eq. 6).

that for similar k_{600} values under the two configurations, the turbulence measured under the chamber was higher than the corresponding free-water measurements. This forcefully demonstrates the contention that FCs overestimate fluxes by turbulence enhancement. A statistical comparison of the least-squared regressions of k_{600} vs. ε_{fw} and ε_{in} ($R^2 = 0.48$, $n = 64$, $p < 0.0001$ and $R^2 = 0.78$, $n = 57$, $p < 0.0001$, respectively) by ANCOVA showed that both the slopes and elevations were significantly different (*F*-test for homogeneity of slopes [$p < 0.0001$] and elevation [$p < 0.0001$]). Again, no differences were observed between the reservoir and lake data.

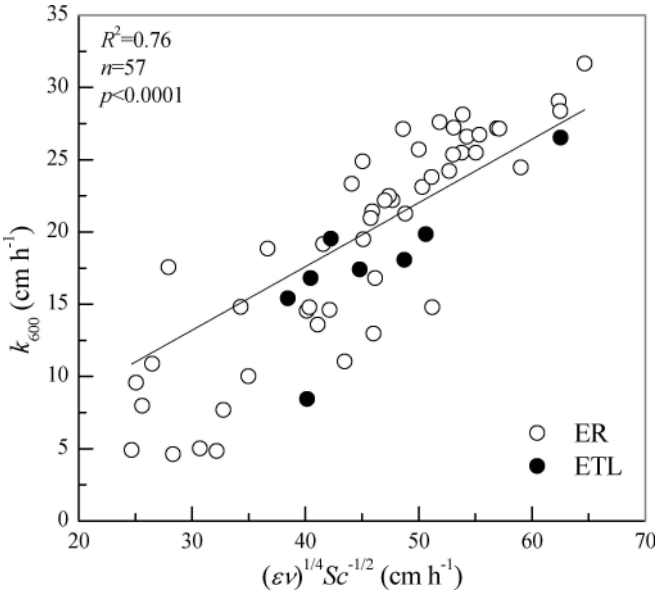

Fig. 4. Relationship between k_{600} predicted by small-eddy model [$(\varepsilon\upsilon)^{1/4}Sc^{-1/2}$] using ε_{in} and measured k_{600} with FC. Solid line represent the linear regression best fit constrained to a 0 intercept [$k_{600} = 0 + 0.43$ (± 0.012) $(\varepsilon\upsilon)^{1/4}Sc^{-1/2}$, $R^2 = 0.76$, $n = 57$, $p < 0.0001$].

To illustrate the extent to which FCs can overestimate gas fluxes, we constructed an overestimation coefficient as the ratio of the measured k_{600} values in the free-water configuration to that predicted from Eq. 6. As a further precautionary measure, we excluded data where the predicted k_{600} was outside the range of values observed in the model development (in our case, below a predicted k_{600} of 1.6 cm h^{-1}). A ratio of unity corresponds to an unbiased prediction, whereas values above 1 imply overestimation. As already implied by the divergent slopes in Fig. 5, Fig. 6 illustrates the highly nonlinear behavior of the overestimation ratio with turbulence. At relatively low turbulence ($< 1.5 \times 10^{-5}$ m^2 s^{-3}, left of 'a' on Fig. 6), FCs can easily overestimate true flux by a several-fold measure. At intermediate turbulence (between 'a' [1.5×10^{-5} m^2 s^{-3}] and 'b' [4×10^{-5} m^2 s^{-3}] on Fig. 6), the mean overestimation ratio is 1.58 ± 0.34 (mean ± SE, $n = 34$). At relatively high turbulence ($> 4 \times 10^{-5}$ m^2 s^{-3}, after 'b' on Fig. 6), overestimation is, on average, less than 50% (1.41 ± 0.31 [mean ± SE, $n = 17$]). The average overestimation ratio can be described by the following equation:

$$\text{Overestimation ratio} = \frac{77.96\ (\pm 7.99) + 13.21\ (\pm 1.74)\log_{10}\varepsilon}{78.22\ (\pm 4.25) + 14.66\ (\pm 1.05)\log_{10}\varepsilon} \quad (7)$$

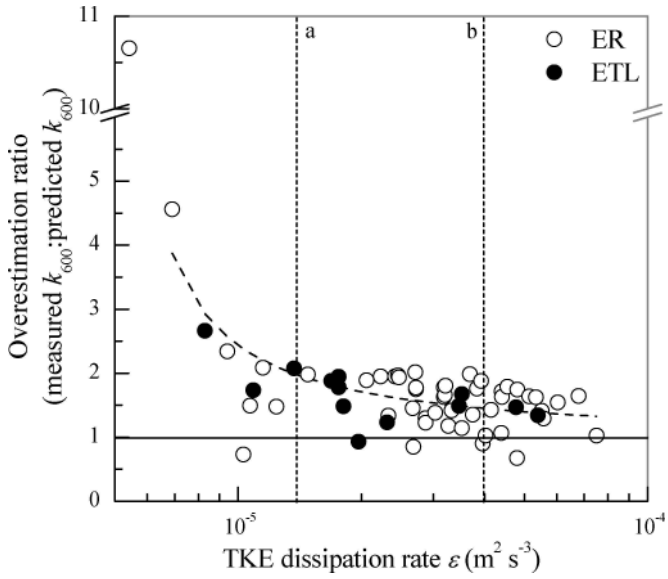

Fig. 6. Overestimation ratio (measured k_{600} : predicted k_{600}) of the FC in relation to the free-water near-surface turbulence measurements (n = 62). Dashed line is the trend of the relationship (Eq. 7). Dotted line separations 'a' and 'b' represent first and second thresholds, respectively. Left of a section represents situations of high overestimation. Between 'a' and 'b' section has a mean overestimation ratio of 1.58 ± 0.34 (mean ± SE, n = 34). After 'b' section represent situations of low overestimation, with a mean of 1.41 ± 0.31 (mean ± SE, n = 17).

Discussion

Relationship between k_{600} *and turbulence*—Many authors have pointed out that near-surface turbulence is a key factor governing gas exchanges across the air–water interface because it constitutes a direct proxy of the physical state of the mass boundary layer (Tokoro et al. 2008). The gas transfer velocity estimation from turbulence has the advantage of being likely quasi-universal among the different system types, regardless of what drives that turbulence. The relationship between near-surface turbulence and gas transfer velocity developed in this study (Fig. 3; Eq. 6) is promising in both its general applicability and its precision (R^2 = 0.78). However, we suggest that this relationship, itself derived from several systems, is probably generally applicable to other temperate or boreal freshwater systems, provided the same turbulence-measurement setup is used, in particular the depth at which turbulence is measured (10 cm). It is likely that the exact parameters of the relationship are dependent on the depth of the turbulence measurements (Zappa et al. 2007). We therefore suggest that further tests should be performed under different conditions before this method can be widely accepted. For practical purposes, we propose that given the consistency of the k_{600}–ε relationship derived above, gas flux could therefore be estimated more simply by measuring turbulence (and deriving k_{600} from Eq. 6) in conjunction with gas partial pressure measurements. This approach would likely be preferable to measuring gas flux directly with a FC, given the biases the FC introduces (*see* discussion below).

The predictive utility of a single turbulence-based model lies not only in its precision but also in its wide application to a variety of systems, from rivers and lakes to reservoirs and estuaries (Zappa et al. 2007; Tokoro et al. 2008). This is a major advantage of k_{600} models based on turbulence over those based on a proxy such as wind speed. As pointed out by Borges et al. (2004) and Guérin et al. (2007), there is strong evidence that the parameters of the wind–k_{600} relationship vary systematically with system size, as demonstrated by the linear trend between the slope of wind–k_{600} relationships and the surface area of the system over which they were developed (*see* fig. 3 in Guérin et al. [2007]). This argument is, however, well known in the literature (Upstill-Goddard et al. 1990; Wanninkhof 1992), and our results support this contention. Using Eq. 7 in conjunction with the observed free-water turbulence allows us to calculate a corrected k_{600} value for each observation. Figure 7 shows the relationship between corrected k_{600} and wind speed for both the ER and ETL data. Both data sets show relatively poor relationships, particularly for ETL, which also had a tendency to have lower gas exchange for any given wind speed. System size could thus be a significant issue when estimating k_{600} from wind speed. It is obvious that the longer (in terms of time and distance) the wind is blowing, the more it will transfer its energy to the surface waters. Thus, we submit that when only wind data are available, wind fetch together with wind speed and duration may be better predictors of surface turbulence conditions than is wind speed alone. Such models have yet to be developed, however, and the major advantage of turbulence-based models is that they can be used regardless of the size of the system.

Figure 7 also compares our corrected k_{600} to wind speed trends from other published relationships. For the same wind speed range, our reservoir data are somewhat smaller than those reported from the Scheldt estuary (Borges et al. 2004), also estimated using FCs. However, our lake values were higher than those predicted by Crusius and Wanninkhof (2003) or those of the Cole and Caraco (1998) relationship, both of which had been developed using SF_6 as a tracer. Differences between FC measurements (our study) and SF_6 (Cole and Caraco 1998; Crusius and Wanninkhof 2003) reside mainly in the temporal and spatial integration scales of the measurements. The FC method usually integrates fluxes in an area of about 0.1 m^2 over less than 30 min (in our case, 10 min), while the SF_6 addition integrates fluxes at the whole-lake scale over periods of a few days. This may in part explain our results being greater than those associated with the oft-cited relationship of Cole and Caraco (1998) because our central sampling point was located at the more wind-exposed area. However, we also had higher k_{600} values compared to values from the study of Guérin et al. (2007), who also used FCs. Although the observed discrepancy could be related to further methodological biases that were not taken into account in our correction factor (e.g., models of FC and time of deployment), it may also involve other as-yet-unidentified environmental factors that influence gas exchanges at low wind speed. These may include thermocline depth, fetch, lake depth, and chemical factors such as

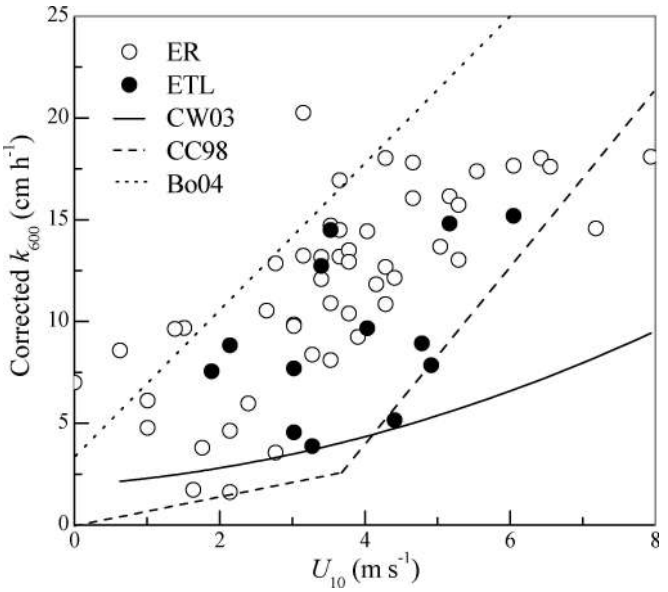

Fig. 7. Corrected k_{600} data plotted against wind speed at 10 m (U_{10}). The dashed line represents the Cole and Caraco (1998) relationship (CC98), the dotted line represents Borges et al. (2004) relationship (Bo04), and the long dashed line represents the Crusius and Wanninkhof (2003) relationship (CW03).

surfactants. Nevertheless, we contend that turbulence variables have the advantage of taking into account the modulating effects of such factors on the turbulence generated by a given wind speed itself (Jonsson et al. 2008).

Small-eddy model—Our results are also useful in evaluating the appropriateness of certain theoretical models to field applications. The small-eddy model states that k_{600} should be proportional to the 0.25 power of ε. Figure 4 shows the relationship between k_{600} predicted from the small-eddy model based on ε_{in} and the measured k_{600} with FC at the same ε_{in} ($k_{600} = 0 + 0.43$ [$\pm$ 0.012], $R^2 = 0.76$, $n = 57$, $p < 0.0001$). Again, we consider this relationship to be valid even if FCs induce artificial turbulence because our turbulence measurements (ε_{in}) were made inside the FC sampling area, thus encompassing the turbulence produced by the chamber. Our results as well as those of other studies demonstrate the universality of the small-eddy model to many types of aquatic systems. Zappa et al. (2007) found a good relationship when combining data from four different systems (rivers to estuaries). Similar results were obtained in a recent study (Tokoro et al. 2008) in marine coastal systems that used the FC method. However, some difference appears between the slopes of these relationships. By rearranging Eq. 2, thus,

$$k_{600} = A(\varepsilon\upsilon)^{1/4} Sc^{-n} \quad (8)$$

the coefficient A represents the slope parameter that explains the difference between relationships. For our study, when separating ER and ETL data, slopes of the least-squared regressions with 0 intercepts are similar ($k_{600} = 0.44$ [$\pm$ 0.01], $R^2 = 0.78$, $n = 49$, $p < 0.0001$ and $k_{600} = 0.39$ [$\pm$ 0.02] $(\varepsilon\upsilon)^{1/4} Sc^{-1/2}$, $R^2 = 0.66$, $n = 8$, $p < 0.0001$, for ER and ETL, respectively). In our case, differences among systems do not affect the applicability of this relationship. However, when comparing our results to those of other studies (Zappa et al. 2007; Tokoro et al. 2008), some differences remain, even if our slope is similar to that of Zappa et al. (2007; $A = 0.43$, $A = 0.419$, respectively).

A solid predictive model to determine air–water gas exchanges using small-eddy model requires that A be parameterized with precision. Several factors may explain differences in parameter A between our study and those of Zappa et al. (2007) and Tokoro et al. (2008), but we suggest that these differences are most likely attributable to differences in the acquisition of the turbulence measurements, which were not taken at the same depth. Because turbulence will dissipate vertically and nonlinearly from the forcing source, sampling depth will be critical when comparing measured k to turbulence-modeled k.

Bias and corrections for FC measurements—Our FC evaluation agrees with those of many other studies that found that fluxes are overestimated when measured by FC methods by perturbing the air–water interface (Kremer et al. 2003; Matthews et al. 2003; Lambert and Fréchette 2005). Tokoro et al. (2008) also measured turbulence inside and outside their FC, but they did not find major disagreements between the two types of measurements. However, their inside chamber measurements were made from an ADV that was fixed on the seafloor, and the near-surface turbulences were extrapolated. FC perturbation is certainly more significant within the first few centimeters from the surface and is therefore likely undetectable from seafloor probe–extrapolated turbulence values.

Our results show that most of the time, the overestimation ratio is under 2 (90% of the data fall between values of 0.67 and 2.05). However, the overestimation caused by FCs is not constant but rather depends strongly on the turbulence regime (Fig. 6). FC introduces a strong bias in calm, low-turbulence waters, where the FC movements on the surface will increase significantly the water movements inside the sampling area (relative to the natural water state). At higher turbulence regimes, when wind waves are added, artificially created turbulence caused by movements of FC on surface waters is relatively less important. Figure 6 illustrates what we consider two important turbulence thresholds: 'a' and 'b.' At very low turbulence (left of 'a'), FC measurements are at high risk for important flux overestimations. On small lakes such as ETL, this water condition corresponds to a wind speed of less than 2–3 m s^{-1}, which is usually frequent. In larger systems such as the ER, this low-turbulence condition is equivalent to a wind speed of less than 1–2 m s^{-1}. At the other end of Fig. 6, threshold 'b' represents the point at which FC measurements are comparatively much more adequate (overestimation less than 50%). This point corresponds to a wind speed of greater than 6.5 m s^{-1} in small systems like ETL, an infrequent situation. In general, our results imply that using FC on small systems will be most

problematic. On reservoirs or very large lakes, the threshold 'b' corresponds to a wind speed of greater than 4–6 m s^{-1}. According to our results at the ER, those conditions are more frequent, thus reducing flux exaggerations considerably. Therefore, our mean overestimation on the reservoir is still about 50%, which is non-negligible. Thus, thresholds in the relationship with wind speed are themselves probably dependent on system size. Consequently, fluxes measured by FC on small lakes (< 2 km^2), which are numerous in Québec, are probably overestimated by a twofold to 10-fold measure.

The overall trend toward FC overestimations in our study is still consistent with the conclusions of Matthews et al. (2003). Their FC overestimations were much more important in calm-water conditions than they were when waves were present at higher wind speeds. However, their hypothesis that this was due to the lack of side walls penetrating the surface is not supported by our data, since our chamber had 6-cm walls extending into the water column. Even if FC designs may influence flux measurements by disturbing differently the air–water interface, further experiments are clearly needed to evaluate the real effect of wall extensions. Although our overestimation trend is a general one, it is important to note that the extent of our absolute overestimation is probably specific to our own particular FC design. FCs with other configurations may overestimate true flux differently. Also, because our model is linear (Fig. 3), extremely low turbulence may still offer some biases, because we could not observe such low turbulence with FCs (hence, our exclusion of data outside the observed range). Theoretically, if water completely stops moving (i.e., $\varepsilon \rightarrow 0$), there will still be gas exchanges across the air–water interface. We suggest that k_{600} values derived from extremely low turbulence ($<5 \times 10^{-6}$ m^2 s^{-3}) values should be interpreted with caution. Moreover, while our system enabled us to examine the artificial turbulence generated by the chamber and therefore allowed us to correct for it, it is still possible that our turbulence measurement system itself generated some additional perturbations (*see* Fig. 1).

When estimating carbon exchanges between water surfaces and the atmosphere, choosing the right k value remained a major challenge. By using a dual series of concurrent flux and turbulence measurements, we have shown that near-surface turbulence can be used effectively to derive robust k values and that the theoretical small-eddy model was well supported by our data. We also showed that while our FC overestimates gas fluxes by up to a 10-fold measure in calm-water conditions, it is likely adequate in more turbulent conditions (i.e., less than 50%). These numbers may be specific to our FC design and may need further testing. Finally, we propose that turbulence-based models are more general and accurate than k–wind relationships, which we contend are largely system specific.

Acknowledgments

We thank Sally MacIntyre and William Shaw for their generous help with turbulence calculations, Darryl Gilpin, John Moses, Gaëlle Derrien and Lisa Fauteux for assistance in the field, and H.S.C. for unwavering guidance. This research was funded by Hydro-Quebec as part of the Eastmain-1 research project and by a discovery grant from the Natural Sciences and Engineering Research Council of Canada (to Y.T.P.).

References

Abril, G., M.-V. Commarieu, A. Sottolichio, P. Bretel, and F. Guérin. 2009. Turbidity limits gas exchange in a large macrotidal estuary. Estuar. Coast. Shelf Sci. **83:** 342–348, doi:10.1016/j.ecss.2009.03.006

Borges, A. V., B. Delille, L.-S. Schiettecatte, F. Gazeau, G. Abril, and M. Frankignoulle. 2004. Gas transfer velocities of CO_2 in three European estuaries (Randers Fjord, Scheldt, and Thames). Limnol. Oceanogr. **49:** 1630–1641.

Calleja, M. L., C. M. Duarte, Y. T. Prairie, S. Agustì, and G. J. Herndl. 2009. Evidence for surface organic matter modulation of air-sea CO_2 gas exchange. Biogeosciences **6:** 1105–1114, doi:10.5194/bg-6-1105-2009

Cole, J. J., and N. F. Caraco. 1998. Atmospheric exchange of carbon dioxide in a low-wind oligotrophic lake measured by the addition of SF_6. Limnol. Oceanogr. **43:** 647–656.

———, and Y. T. Prairie. 2009. Dissolved CO_2, p. 30–34. *In* G. E. Likens [ed.], Encyclopedia of inland waters. Elsevier.

———, and others. 2007. Plumbing the global carbon cycle: Integrating inland waters into the terrestrial carbon budget. Ecosystems **10:** 171–184, doi:10.1007/s10021-006-9013-8

Crusius, J., and R. Wanninkhof. 2003. Gas transfer velocities measured at low wind speed over a lake. Limnol. Oceanogr. **48:** 1010–1017.

Dankwerts, P. V. 1951. Significance of liquid-film coefficients in gas adsorption. Ind. Eng. Chem. **43:** 1460–1467, doi:10.1021/ie50498a055

Eugster, W., G. Kling, T. Jonas, J. P. McFadden, A. Wüest, S. MacIntyre, and F. S. Chapin, III. 2003. CO_2 exchange between air and water in an Arctic Alaskan and midlatitude Swiss lake: Importance of convective mixing. J. Geophys. Res. **108:** 4362, doi:10.1029/2002JD002653

Frankignoulle, M. 1988. Field measurements of air-sea CO_2 exchange. Limnol. Oceanogr. **33:** 313–322, doi:10.4319/lo.1988.33.3.0313

Frew, N. M., J. C. Goldman, M. R. Dennett, and A. S. Johnson. 1990. Impact of phytoplankton-generated surfactants on air-sea gas exchange. J. Geophys. Res. **95:** 3337–3352, doi:10.1029/JC095iC03p03337

Frost, T., and R. C. Upstill-Goddard. 2002. Meteorological controls of gas exchange at a small English lake. Limnol. Oceanogr. **47:** 1165–1174.

Guérin, F. F., and others. 2007. Gas transfer velocities of CO_2 and CH_4 in a tropical reservoir and its river downstream. J. Mar. Syst. **66:** 161–172, doi:10.1016/j.jmarsys.2006.03.019

Ho, D. T., L. F. Bliven, R. Wanninkhof, and P. Schlosser. 1997. The effect of rain on air-water gas exchange. Tellus **49:** 149–158, doi:10.1034/j.1600-0889.49.issue2.3.x

———, F. Veron, E. Harrison, L. F. Bliven, N. Scott, and W. R. McGillis. 2007. The combined effect of rain and wind on air-water gas exchange: A feasibility study. J. Mar. Syst. **66:** 150–160, doi:10.1016/j.jmarsys.2006.02.012

Jonsson, A., J. Aberg, A. Lindroth, and M. Jansson. 2008. Gas transfer rate and CO_2 flux between an unproductive lake and the atmosphere in northern Sweden. J. Geophys. Res. **113:** G04006, doi:10.1029/2008JG000688

Kitaigorodskii, S. A., M. A. Donelan, J. L. Lumley, and E. A. Terray. 1983. Wave-turbulence interactions in the upper ocean. Part II: Statistical characteristics of wave and turbulent components of the random velocity field in the marine surface layer. Journal of Oceanography **13:** 1988–1999.

Kremer, J. N., A. Reischauer, and C. D'avanzo. 2003. Technical note: Conditions for using the floating chamber method to estimate air-water gas exchange. Estuaries **26:** 985–990, doi:10.1007/BF02803357

LAMBERT, M., AND J.-L. FRÉCHETTE. 2005. Analytical techniques for measuring fluxes of CO_2 and CH_4 from hydroelectric reservoirs and natural water bodies, p. 37–60. *In* A. Tremblay, L. Varfalvy, C. Roehm and M. Garneau [eds.], Greenhouse gas emissions—fluxes and processes: Hydroelectric reservoirs and natural environments. Springer.

LAMONT, J. C., AND D. S. SCOTT. 1970. Eddy cell model of mass transfer into the surface of a turbulent liquid. AIChE J. **16:** 513–519, doi:10.1002/aic.690160403

LUMLEY, J. L., AND E. A. TERRAY. 1983. Kinematics of turbulence convected by a random wave field. J. Phys. Oceanogr. **13:** 2000–2007, doi:10.1175/1520-0485(1983)013<2000:KOTCBA>2.0.CO;2

MACINTYRE, S., R. WANNINKHOF, AND J. P. CHANTON. 1995. Trace gas exchange across the air-water interface in freshwater and coastal marine environments, p. 52–97. *In* P. A. Matson and R. C. Harriss [eds.], Biogenic trace gases: Measuring emissions from soil and water. Blackwell.

MATTHEWS, C. J. D., V. L. ST. LOUIS, AND R. H. HESSLEIN. 2003. Comparison of three techniques used to measure diffusive gas exchange from sheltered aquatic surfaces. Environ. Sci. Technol. **37:** 772–780, doi:10.1021/es0205838

MCKENNA, S. P., AND W. R. MCGILLIS. 2004. The role of free-surface turbulence and surfactants in air-water gas transfer. Int. J. Heat Mass Transfer **47:** 539–553, doi:10.1016/j.ijheatmasstransfer.2003.06.001

REPO, M. E., J. T. HUTTUNEN, A. V. NAUMOV, A. V. CHICHULIN, E. D. LAPSHINA, W. BLEUTEN, AND P. J. MARTIKAINEN. 2007. Release of CO_2 and CH_4 from small wetland lakes in western Siberia. Tellus **59:** 788–796, doi:10.1111/j.1600-0889.2007.00301.x

SCHLADOW, S. G., M. LEE, B. E. HÜRZELER, AND P. B. KELLY. 2002. Oxygen transfer across the air-water interface by natural convection in lakes. Limnol. Oceanogr. **47:** 1394–1404.

SOUMIS, N., R. CANUEL, AND M. LUCOTTE. 2008. Evaluation of two current approaches for the measurement of carbon dioxide diffusive fluxes from lentic ecosystems. Environ. Sci. Technol. **42:** 2964–2969, doi:10.1021/es702361s

STAUFFER, R. E. 1980. Wind power time series above a temperate lake. Limnol. Oceanogr. **25:** 513–528, doi:10.4319/lo.1980.25.3.0513

TERRAY, E. A., AND OTHERS. 1996. Estimates of kinetics energy dissipation under breaking waves. J. Phys. Oceanogr. **26:** 792–807, doi:10.1175/1520-0485(1996)026<0792:EOKEDU>2.0.CO;2

TOKORO, T., AND OTHERS. 2008. High gas-transfer velocity in coastal regions with high energy-dissipation rates. J. Geophys. Res. **113:** C11006, doi:10.1029/2007JC004528

UPSTILL-GODDARD, R. C., A. J. WATSON, P. S. LISS, AND M. I. LIDDICOAT. 1990. Gas transfer velocities in lakes measured with SF_6. Tellus **42:** 364–377, doi:10.1034/j.1600-0889.1990.t01-3-00006.x

WANNINKHOF, R. 1992. Relationship between wind speed and gas exchange over the ocean. J. Geophys. Res. **97:** 7373–7382, doi:10.1029/92JC00188

———, AND W. R. MCGILLIS. 1999. A cubic relationship between air-sea CO_2 exchange and wind speed. Geophys. Res. Lett. **26:** 1889–1892, doi:10.1029/1999GL900363

ZAPPA, C. J., W. E. ASHER, A. T. JESSUP, J. KLINKE, AND S. R. LONG. 2004. Microbreaking and the enhancement of air-water transfer velocity. J. Geophys. Res. **109:** C08S16, doi:10.1029/2003JC001897

———, P. A. RAYMOND, E. A. TERRAY, AND W. R. MCGILLIS. 2003. Variation in surface turbulence and the gas transfer velocity over a tidal cycle in a macro-tidal estuary. Estuaries **26:** 1401–1415, doi:10.1007/BF02803649

———, AND OTHERS. 2007. Environmental turbulent mixing controls on air-water gas exchange in marine and aquatic systems. Geophys. Res. Lett. **34:** L10601, doi:10.1029/2006GL028790

Associate editor: Christopher M. Finelli

Received: 28 July 2009
Accepted: 01 March 2010
Amended: 29 April 2010